

# Characterization and Functional Analysis of CD44v6.CAR T Cells Endowed with a New Low-Affinity Nerve Growth Factor Receptor-Based Spacer

Anna Stornaiuolo,<sup>1,†</sup> Barbara Valentinis,<sup>1,†</sup> Camilla Sirini,<sup>1-3</sup> Cinzia Scavullo,<sup>1</sup> Claudia Asperti,<sup>1,‡</sup> Dan Zhou,<sup>1</sup> Yeny Martinez De La Torre,<sup>1</sup> Stefano Corna,<sup>1</sup> Monica Casucci,<sup>2</sup> Simona Porcellini,<sup>1,‡</sup> and Catia Traversari<sup>1,\*</sup>

<sup>1</sup>Research Department, AGC Biologics SpA (Formerly MolMed SpA), Milan, Italy; <sup>2</sup>Innovative Immunotherapies Unit, Division of Immunology, Transplantation and Infectious Diseases, IRCSS San Raffaele Scientific Institute, Milan, Italy; and <sup>3</sup>Vita-Salute San Raffaele University, Milan, Italy.

<sup>†</sup>These authors contributed equally to this work.

<sup>‡</sup>Present address: San Raffaele Telethon Institute for Gene Therapy, IRCCS San Raffaele Scientific Institute, Milan, Italy.

Effectiveness of adoptively transferred chimeric antigen receptor (CAR) T cells strongly depends on the quality of CAR-mediated interaction of the effector cells with the target antigen on tumor cells. A major role in this interaction is played by the affinity of the single-chain variable fragment (scFv) for the antigen, and by the CAR design. In particular, the spacer domain may impact on the CAR T cell function by affecting the length and flexibility of the resulting CAR. This study addresses the need to improve the manufacturing process and the antitumor activity of CD44v6-specific CAR T cells by defining the optimal structure of a spacer region derived from the extracellular domain of the human low-affinity nerve growth factor receptor (LNGFR). We tailored the LNGFR spacer to modulate CAR length to efficiently recognize distal or proximal epitopes and to allow selection of transduced CAR T cells by the use of clinical-grade validated manufacturing systems. The different LNGFR spacers investigated in this study are responsible for the generation of CAR T cells with a different memory phenotype, which is mainly related to the level of CAR expression and the extent of the associated tonic signaling. In particular, the CD44v6-NWN2.CAR T cells are enriched in central memory cells and show improved *in vitro* functions in terms of killing capability, and *in vivo* antitumor activity against hematological and solid tumors. Clinical Trial Registration numbers: clinical.trial.gov NCT04097301; ClinicalTrials.gov, NCT00423124.

**Keywords:** CAR T, CD44v6, spacer, adoptive cell therapy, solid tumor

## INTRODUCTION

CHIMERIC ANTIGEN RECEPTORS (CARs) are antigen-specific recombinant molecules that, expressed on T lymphocytes (CAR T), reprogram their specificity and function thus allowing the generation of a large number of tumor-specific effectors for adoptive immunotherapy.<sup>1,2</sup> CAR T cell therapy represents a true “vital drug” that has immediate and specific effects against cancer cells, and that may potentially provide long-term protection due to the persistence of immune memory cells.<sup>3,4</sup>

CARs are constructed by fusing an extracellular antigen-binding portion, commonly the single-chain variable fragment (scFv) of a tumor-reactive monoclonal

antibody (mAb), with intracellular activation units, usually the CD3 $\zeta$ -chain, coupled with costimulatory endodomains from either CD28 or 41BB.<sup>5</sup> The expression of CAR molecules in T lymphocytes is usually obtained by transduction with viral vectors. This involves T cell pre-activation and *in vitro* expansion, procedures that may modify T cell differentiation, limiting T cell reactivity and functionality. It has been reported that CARs with different binding strengths and signaling properties can modulate CAR T cell expansion, persistence, and activation within the tumor microenvironment, features that radically change the efficacy and safety of tumor-targeted CAR T cell therapy.<sup>6,7</sup>

\*Correspondence: Dr. Catia Traversari, Research Department, AGC Biologics SpA (Formerly MolMed SpA), Milan 20132, Italy. E-mail: ctraversari@agcbio.com

© Anna Stornaiuolo *et al.*, 2021; Published by Mary Ann Liebert, Inc. This Open Access article is distributed under the terms of the Creative Commons Attribution Noncommercial License [CC-BY-NC] (<http://creativecommons.org/licenses/by-nc/4.0/>) which permits any noncommercial use, distribution, and reproduction in any medium, provided the original author(s) and the source are cited.

The properties of CAR-antigen interaction depend not only on the scFv affinity but also on the presence of a spacer that connects the scFv to the transmembrane domain of the CAR. In fact, it has been reported that spacer length, influencing CAR interaction with epitopes that can be distal or proximal to the cell membrane, can have an effect on the overall functional properties of CAR T cells.<sup>8,9</sup> Recently, we described an innovative spacer<sup>10</sup> based on the extracellular domains of the human low-affinity nerve growth factor receptor (LNGFR; P08138, TNR16\_HUMAN) (Fig. 1A). The LNGFR spacer behaves as a marker protein allowing the selection of transduced CAR T cells during manufacturing by the use of clinical-grade validated systems,<sup>11–13</sup> as well as the *in vivo* monitoring of CAR T cells.<sup>14</sup> The antitumor efficacy of LNGFR-enriched CAR T cells specific for dif-

ferent target antigens, including the v6 variant of the adhesion molecules CD44 (CD44v6), was validated in clinically relevant *in vitro* assays and *in vivo* xenograft tumor models.<sup>15</sup> In particular, the CD44v6.CARs containing LNGFR spacers of different lengths<sup>10</sup> are second-generation CARs directed against the CD44v6 antigen. They are endowed with the transmembrane and intracellular signaling domains of the human costimulatory CD28, and the intracellular signaling domain of the human CD3 $\zeta$ -chain (Fig. 1A). Recently, the CD44v6.CAR endowed with the longer LNGFR spacer has been used in a phase I/IIa clinical trial to assess the safety, efficacy, and feasibility of CD44v6.CAR T cell immunotherapy in patients affected by CD44v6-positive acute myeloid leukemia (AML) and multiple myeloma (MM) (clinical trial.gov NCT04097301).

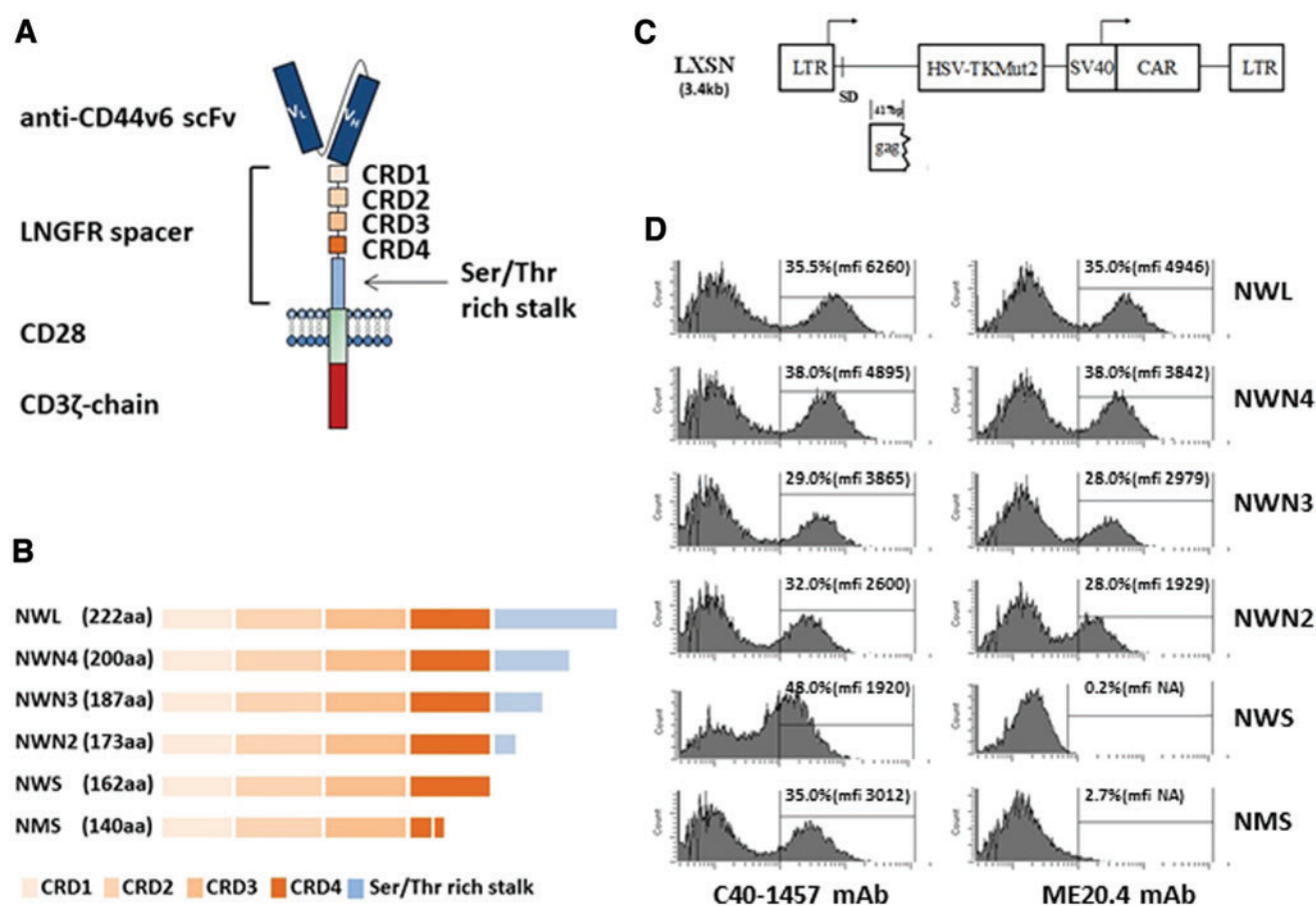


**Figure 1.** Features of the CAR constructs. **(A)** Schematic structure of the CD44v6-LNGFR CAR. The CAR contains a CD44v6 binding domain (anti-CD44v6 scFv), the LNGFR spacer (four TNFR-Cys domains [CRDs] and the serine/threonine-rich stalk), the transmembrane and costimulatory domain of CD28, and the intracellular domain of CD3 $\zeta$  chain. **(B)** Schematic structure of the different LNGFR spacers. The LNGFR wild-type long spacer (NWL) contains the four CRD and the entire serine/threonine-rich stalk. The optimized LNGFR spacers N4 (NWN4), N3 (NWN3), and N2 (NWN2) contain the four CRDs and the first 38, 25, and 11 amino acids of the serine/threonine-rich stalk, respectively. The NWS spacer contains only the four CRDs, while the NMS spacer contains the first three CRDs and a deleted version of the CRD4.<sup>10</sup> **(C)** Schematic representation of the retroviral vector construct LTK-SCD44v6-CAR derived from Moloney murine leukemia virus. The construct contains the transcriptional promoter 5' viral long terminal repeat (5'LTR), the viral sequence including the packaging signal and *gag* gene ( $\Psi$ + *gag*), the polynucleotide coding for the suicide gene *HSV-TK Mut2*, the transcriptional promoter SV40 (Simian virus 40), the CD44v6 CAR, and the 3' viral long terminal repeat (3'LTR). **(D)** Characterization of the binding of the two anti LNGFR Abs, C40-1457 and ME20.4, to the CARs expressed by CEM A301 cells transduced with the different CAR constructs. Cells were analyzed at day 3 of culture. Percentage of transduction and MFI is shown in the *inset*. CAR, chimeric antigen receptor; LNGFR, low-affinity nerve growth factor receptor; MFI, median fluorescence intensity; scFv, single-chain variable fragment. Color images are available online.

CD44 is a glycoprotein physiologically expressed on the surface of many mammalian cells, which includes endothelial and epithelial cells, fibroblasts, keratinocytes, and leukocytes.<sup>16</sup> Human CD44 splice variants originate by alternative splicing of nine variable exons in different combinations. Splice variants containing variable exon 6 (*i.e.*, CD44v6) have been implicated in tumorigenesis, tumor cell invasion and metastasis,<sup>17</sup> and are expressed in several tumor types,<sup>18</sup> whereas on normal epithelial tissues, detectable CD44v6 expression has been reported only in skin and oral mucosa, although at considerably lower levels than in tumors.<sup>19</sup> In the CD44v6 isoforms, variable exon 6 can be associated with different patterns of variable exons. This alternative splicing generates isoforms in which the variable exon 6 can be distal or proximal to the cell membrane.

In this study, we tailored the spacer region to modulate CAR length to efficiently recognize distal or proximal epitopes, with the final aim of improving CD44v6.CAR T functionality, including preservation of a differentiation status suitable for effective *in vivo* antitumor activities.

## MATERIALS AND METHODS

### LNGFR-spaced CD44v6 CAR constructs

The CD44v6-NWL.CAR consists of a CD44v6 binding domain, the LNGFR wild-type long spacer that includes the entire extracellular domain of the human LNGFR, the transmembrane and costimulatory domain of CD28, and the intracellular domain of CD3 $\zeta$  chain. In the CD44v6-NWS and CD44v6-NMS CARs, the LNGFR spacer was deleted of the entire serine/threonine-rich stalk. Moreover, in the CD44v6-NMS.CAR, the LNGFR spacer carries also a deletion of the TNFR-Cys domains that prevents recognition by the anti-LNGFR mAb ME20.4.<sup>10</sup> The three new chimeras, NWN4, NWN3, and NWN2, were constructed starting from the CD44v6-NWS.CAR construct by adding to the four TNFR-Cys domains, the fragments of 38, 25, and 11 amino acids of the serine/threonine-rich stalk, respectively. This cloning strategy allows to preserve the mAb ME20.4 epitope that is lost in the CD44v6-NMS.CAR.<sup>10</sup> The cloning was performed using the *PmlI* and *NotI* restriction enzymes cutting in the LNGFR sequence and at 3' of the CD3 $\zeta$  chain, respectively. The region codifying for the NWN4, NWN3, and NWN2 chimeras was synthesized by Eurofins (Vimodrone, Italy) and cloned in the *PmlI/NotI* of the CD44v6-NWS.CAR, generating the corresponding constructs. The CD44v6 binding domain is constituted by the scFv of the humanized mAb BIWA-8<sup>20</sup> specific for the CD44v6 antigen.

### Cloning of CD44v6 transcripts

Peripheral blood mononuclear cells (PBMCs) were activated with TransAct (Miltenyi Biotec) for 2 days to selectively stimulate T cells. CD44v6 expression at day 2

was monitored and total RNA was isolated with the RNeasy Mini Kit (QIAGEN) from  $4 \times 10^6$  cells. The same kit was used to isolate total RNA from THP1 cells ( $4 \times 10^6$  cells). SuperScript First-Strand Synthesis System (Invitrogen) with random primers was used for reverse transcriptase (RT)-PCRs with 3  $\mu$ g of total RNA. For PCR amplification of the cDNA corresponding to CD44v6 isoforms, the following specific primer pairs for v6 exon and for the standard exons were used:

CD44(5')FW (5'-ATGGACAAGTTTTGGTGGCAGCAGCCTG-3'),

CD44(3')rev (5'-TTACACCCCAATCTTCATGTCCA CATTCTG-3'),

CD44(v6)FW (5'-TCCAGGCAACTCCTAGTAGTAC AACGG-3'), CD44(v6)rev (5'-CAGCTGTCCCTGTTGT CGAATGGG-3').<sup>21</sup> The PCR amplified the CD44v6 cDNA in two steps: with the primer pair CD44(5')FW/CD44(v6)rev was amplified the region corresponding to the 5' standard region plus the variable regions containing the v6 exon; with the primer pair CD44(v6)FW/CD44(3')rev was amplified the region corresponding to the 3' standard region plus the variable region containing the v6 exon. The 5' and 3' fragments of the *CD44v6* gene from lymphocytes or from THP1 cell line were then joined together using the *EcoRV* restriction enzyme present in the v6 exon to form the complete open reading frame. The location of the primers is depicted in Fig. 7A. The cDNA were then sequenced by Bio-Fab Research (Rome, Italy).

### Retroviral vector design and production

LXSN retroviral vector<sup>22</sup> (GenBank Accession No. 28248), carrying the *HSV-TK Mut2* suicide gene, was used to generate retroviral vectors for the expression of the different CARs. This vector carried the *HSV-TK Mut2* gene under the transcriptional control of the viral 5'LTR promoter and an internal expression cassette with the SV40 promoter driving the expression of the different CD44v6.CARs. The same cloning strategy was applied to generate the control vector expressing the CAR specific for CD19 antigen (CD19-NWL.CAR) and *HSV-TK Mut2* suicide gene.

The two CD44v6 isoforms were cloned in the pMXs retroviral vector to generate pMXs-CD44v6(v6) and pMXs-CD44v6(v6-v10).

### Generation of CAR-engineered T cells

PBMCs from healthy donors were isolated by density gradient centrifugation (Lymphoprep; Fresenius). PBMCs were cultured in Xvivo 15 w/o gentamicin and phenol red (Lonza) supplemented with 3% human plasma AB (Kendron), 100 U/mL penicillin and streptomycin (Lonza), 2 mM L-glutamine (Lonza), and 100 U/mL MACS GMP recombinant IL7 and 200 U/mL MACS GMP recombinant IL15 (Miltenyi Biotec). PBMCs were activated with CD3/CD28 magnetic beads (Dyna, Invitrogen) or TransAct

(Miltenyi Biotec) for 2 days to selectively stimulate T cells. Activated cells were transduced with retroviral vectors for CD44v6.CAR and CD19.CAR expression, in the presence of RetroNectin (Takara) for 18–20 h at 37°C. Cells were cultured and expanded until day 6 for purification of LNGFR expression. Immunoselection was performed with the PE-labeled anti-LNGFR C40-1457 mAb followed by anti-PE MicroBeads (Miltenyi Biotec) or with two well-established clinically validated processes based on the use of the anti-LNGFR (*i.e.*, anti-CD271) mAb Me20.4. The one-step process involves the use of Me20.4 coupled to MicroBeads (CD271-LS MicroBeads; Miltenyi Biotec),<sup>13</sup> whereas in the two-step protocol, incubation with mAb Me20.4 is followed by sheep anti-mouse IgG1-coated magnetic beads<sup>11,12</sup> (Dynabeads M-450; Dynal AS, Oslo, Norway). At the end of the selection process, LNGFR-positive cells (*i.e.*, CAR T cells) were expanded and then frozen at day 10 of culture. For some experiments, CAR T were differentiated *in vitro* with IL2 (100 U/mL) and OKT-3 (30 ng/mL) and their memory phenotype was analyzed after 10 days of culture by CD45RA and CD62L analysis.

### Cell lines

The following CD44v6-positive cell lines were used: MR232, lung carcinoma,<sup>23</sup> IGROV-1, ovarian adenocarcinoma (NCI tumor repository), THP1, human monocytic leukemia (ATCC), and MM1S, myeloma (ATCC). As CD44v6-negative cell lines, MOLT 4, lymphoblastic acute leukemia (ATCC), and BV-173, B cell precursor leukemia,<sup>24</sup> were used.

### Flow cytometry

T cells were stained with a panel of antibodies, including monoclonal mouse anti-human CD271, CD3, CD45, CD4, CD8, CD45 RA, CD62L, HLADR, PD1, CD25, TIM3, and LAG3 (BD Biosciences). Tumor cell lines were stained with the anti-human CD44v6 Ab (BD Biosciences). All samples were acquired with an FACSCanto™ system (BD Biosciences), and analyzed using DIVA software. The memory differentiation phenotype and the exhaustion marker of CAR T cells were analyzed on the CD3<sup>+</sup> gated population of CAR T cells.

### Western immunoblotting

CAR T cells were washed twice with ice-cold PBS, and lysed in RIPA buffer (1% Triton X-100, 0.5% sodium deoxycholate, 0.1% SDS, 1 mM EDTA, 1% NP-40, 150 mM NaCl, and 50 mM Tris-HCl, pH 8.0), supplemented with protease inhibitors (CØmplete, EDTA-free, Roche; 5 µM Pepstatin A) and phosphatase inhibitors (Phospho Stop, Roche, and 1 mM sodium orthovanadate). Equal amounts of total protein were subjected to sodium dodecyl sulfate/polyacrylamide gel electrophoresis (SDS-PAGE) and transferred to 0.4 µm nitrocellulose mem-

branes (Schleicher & Schuell, BioScience, DE) for subsequent immunoblotting. To analyze cell surface proteins, CAR T cells were biotinylated before lysis. Briefly, CAR T cells were washed twice with ice-cold PBS, containing 1 mM MgCl<sub>2</sub>, 0.1 mM CaCl<sub>2</sub>, pH8.0 (Buffer A), and incubated with EZ-Link Sulfo-NHS-LC-Biotin (Thermo Scientific) at a final 0.5 mg/mL concentration, at 4°C for 30 min with gentle agitation. The biotinylation reaction was stopped by removing the biotin and washing three times with the buffer A containing 100 mM glycine. Then cells were rinsed with cold PBS and lysed in RIPA lysis buffer supplemented with protease and phosphatase inhibitors. Equal amounts of total lysates were incubated with washed NeutrAvidin agarose resin (Thermo Scientific) at 4°C for 1 h, and then, after removing the first supernatant (unbound fraction), were washed with RIPA buffer 5 times. Biotinylated proteins were released adding 50 µL of reducing 2×SDS-PAGE loading buffer by heating at 99°C for 10 min and centrifuging at 13,000 rpm for 2 min to collect the supernatant. Pull-down biotinylated proteins were resolved and immunoblotted by Western blot together with total lysates, and unbound fraction (both 1/10 of total lysates used for PD). To analyze the presence of covalent-bound homodimers, total lysates were heated at 99°C for 10 min with 2×SDS-PAGE Loading Buffer w/o β-mercaptoethanol (nonreducing condition), and then resolved by SDS-PAGE. Immunoblotting was performed by blocking the membranes in TBST (0.1% Tween in TBS) containing 5% nonfat dry milk (Merck Millipore, city, DE) for 1 h, at RT, followed by incubation with the CD3-ζ chain Ab (E-3; Santa Cruz Biotech.), or the anti phospho-CD3-ζ chain (pTyr142) (K25-407.69; BD Biosciences), overnight, at 4°C. The blots were then incubated with the anti-mouse horseradish peroxidase-conjugated antibodies (GE Healthcare, city, WI, USA) and developed using the ECL system (GE Healthcare). On the same membrane, after stripping, immunoblots with actin (Sigma-Aldrich), calnexin (Santa Cruz Biotech), or LNGFR (Me20.4) Abs were performed as loading control.

### Cytokine production and CD107a degranulation assays

Degranulation, measured by cell surface modulation of CD107a<sup>25</sup> and intracellular cytokine production (TNF-α and IFN-γ), was analyzed by flow cytometry of CAR T cells incubated with different target cells. Briefly, CD44v6.CAR T and CD19.CAR T cells from different donors, at day 11–15 after the initial stimulation, were left untreated or stimulated with target cells at the ratio of 1:1. Anti-CD107a Ab (Miltenyi) and monensin and brefeldin (BD Biosciences) were added during the incubation period. As positive control, CAR T cells were stimulated with 10 ng/mL phorbol myristate acetate (PMA; Sigma) and 1 µg/mL ionomycin (IONO; Sigma). After 5 h of incubation, cells were stained with anti-CD3 mAb (BD

Bioscience) and Viability Stain 510 (BD Bioscience), fixed, permeabilized (Cytotfix/Cytoperm kit, following the manufacturer's instruction; BD Bioscience), and then stained for intracellular cytokines with TNF- $\alpha$ - and IFN- $\gamma$  (BD Bioscience)-specific Abs. Cells were analyzed by flow cytometry, and viable CD3<sup>+</sup>/CD4<sup>+</sup> or CD3<sup>+</sup>/CD8<sup>+</sup> cells were analyzed for CD107a, TNF- $\alpha$ , and IFN- $\gamma$  expression. The percentage of positive CAR T cells incubated alone (always <5%) was subtracted to the percentage of positive CAR T cells stimulated with the different targets or PMA/IONO.

### T cell killing assays

Luciferase expressing cell lines were cocultured in RPMI with CD44v6.CAR and control CD19.CAR-transduced T cells, at E:T ratio of 1:1, 1:5, and 1:10 in flat, transparent-bottomed, black 96-well plates. Cocultures were analyzed for bioluminescence 5–24 h later as RLU (relative light unit) at the Tecan, Nplex. The cytotoxic activity was calculated as follows:

100 – [(number of live target cells in the presence of CAR T/number of live target cells in the absence of CAR T) × 100]. Using the MOLT-4 cell lines expressing the cloned CD44v6 isoforms, the killing assay was carried out labeling the target cells with carboxyfluorescein diacetate succinimidyl ester (CFSE; E-Bioscience), and coculturing them with the CAR T cells. After 5 h of incubation, live cells were analyzed by FACS adding Flow-Count Fluorospheres (Beckman Coulter), to read a fixed number of events, and 7-amino-actinomycin D (7-AAD; BD Bioscience), as a marker of mortality. The cytotoxic activity was calculated as above.

### In vivo xenograft models

Experimental protocols were approved by the Institutional Animal Care and Use Committee of San Raffaele Scientific Institute (IACUC 725). NOD.Cg-Prkdcscid Il2rgtm1Wjl/SzJ (NSG) transgenic mice of 8 weeks of age were provided by Charles River Laboratories. Mice were infused with  $1.5 \times 10^6$  CD44v6<sup>+</sup> THP-1 leukemia cells and, after 13 days, treated with the different CD44v6.CAR T cells (NWL, NWN2) or with T cells expressing a control CD19-NWL.CAR. Forty days later, mice were sacrificed and their liver weighted, as a measure of tumor burden. In a second murine model,<sup>15</sup> mice were injected subcutaneously with  $0.3 \times 10^6$  IGROV-1 tumor cells. At day 7, mice received, via tail vein injection, CAR-transduced T cells. Five to eight mice per group were used.

## RESULTS

### Construction of CD44v6 CARs bearing different spacers

The CD44v6.CAR, currently under clinical development for the treatment of AML and MM patients (clinical

trial.gov NCT04097301), incorporates as spacer the original extracellular domain of the human LNGFR (herein named NWL for LNGFR wild-type long). The NWL spacer, as shown in Fig. 1A, contains four TNFR cysteine-rich domains (CRD) and a serine/threonine-rich stalk.<sup>10</sup> We generated three new variants (NWN) of this spacer, the NWN4, NWN3, and NWN2 chimeras, which comprise the CRD and 38, 25, and 11 amino acids of the serine/threonine-rich stalk, respectively, as reported in Materials & Methods and Fig. 1B.

The polynucleotides encoding the different CD44v6.CAR NWN-chimeras, and the NMS and NWS variants developed by Casucci *et al.*,<sup>10</sup> were cloned into the LXS retroviral vector (Fig. 1C), already used in several clinical studies of *ex vivo* gene therapy<sup>12,26</sup> along with the *HSV-TK Mut2* suicide gene.<sup>12</sup> Viral supernatants were produced in the PG13 packaging cell line, as detailed in M&M, and titrated detecting CAR expression on transduced CEM A301 cells with the anti-LNGFR mAb C40-1457 (hereafter C40). CAR-expressing CEM A301 cells were also analyzed for the presence of the epitope recognized by ME20.4 mAb, which enables to efficiently enrich CAR T cells through validated clinical-grade technologies for manufacturing of standardized CAR T cell products with narrowed variability.<sup>11–13</sup> As shown in Fig. 1D, all three new CD44v6.CARs (NWN4, NWN3, and NWN2) were stained by mAb ME20.4, whereas the shorter variants NWS and NMS CD44v6.CAR<sup>10</sup> were not recognized.

### CAR expression, immune-selection, and memory phenotype of T lymphocytes transduced with CD44v6 CARs

Surprisingly, despite their staining with mAb ME20.4, CD44v6-NWN2.CAR T cells could not be purified with the clinically validated ME20.4-based technology (CliniMACS CD271-LS MicroBeads; Miltenyi).<sup>13</sup> However, in line with the results reported in Fig. 1D, CAR T cells endowed with both the NMS and NWN2 spacers were efficiently selected to pure populations of CAR-expressing cells, by the C40-PE mAb followed by anti-PE coupled MicroBeads (Supplementary Fig. S1).

To investigate the discrepancy between staining and selection of NWN2-based CAR T cells with ME20.4 mAb, we relied on a two-step method using mAb ME20.4 followed by selection with sheep anti-mouse IgG1-coated magnetic beads, which is a clinically validated selection process.<sup>11</sup> As reported in Fig. 2A, CD44v6-NWN2.CAR T cells were efficiently selected to purity (90%). The yield of the two-step selection was comparable for NWL and NWN2 CAR T cells (40% and 33%, respectively), and slightly more efficient with respect to the one-step process (40% vs. 27% for the NWL CAR T cells). The inability to select the NWN2-expressing cells with the one-step procedure could be due to the low affinity of the ME20.4 mAb-MicroBead complex (*i.e.*, the CD271-LS MicroBead

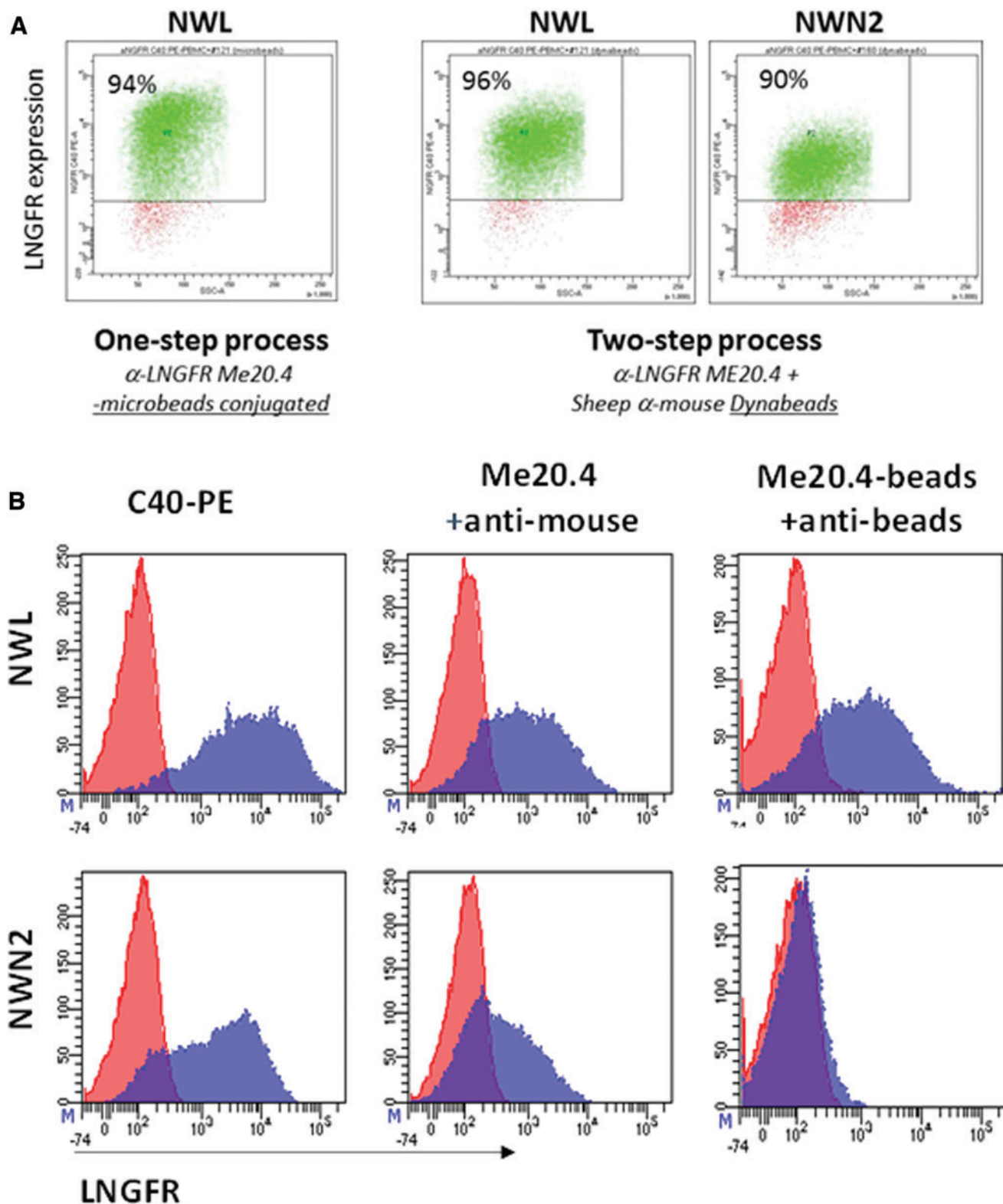


**Figure 2.** Immune-selection of CAR T cells. **(A)** CAR T cells endowed with NWL and NWN2 spacers were immune-selected by the use of either a single-step protocol with the mAb ME20.4 coupled to magnetic MicroBeads (CliniMACS CD271-LS MicroBeads; Miltenyi), or by a two-step method using mAb ME20.4 followed by selection with beads conjugated to anti-mouse antibodies (Dynabeads; Dynal). Both immunoselection processes allowed the isolation of highly enriched (>90%) populations of CAR T cells endowed with NWL spacer, whereas CD44v6-NWN2.CAR T were purified only with the two-step method. **(B)** Pure populations of CAR T cells expressing the NWL or the NWN2 CAR constructs were stained with (1) the anti-LNGFR mAbs C40-PE (*left panels*); (2) the ME20.4 mAb followed by an anti-mouse-PE (*middle panels*); and (3) the ME20.4 mAb coupled to MicroBeads followed by an anti-MicroBead-PE (*right panels*). NWL expressing CAR T cells are recognized by all the combinations tested (*upper panels*). Concerning the NWN2 construct (*lower panels*), ME20.4 mAb is able to bind the transduced cells and can be in turn recognized by an anti-mouse mAb, thus justifying the successful selection obtained with the two-step procedure. On the contrary, when directly coupled to the MicroBeads, the ME20.4 mAb is no more able to bind the NWN2.CAR. mAb, monoclonal antibody. Color images are available online.

reagent) or due to its total inability to interact with the epitope. Pure populations of C40-selected CAR T cells expressing the NWL or the NWN2 CAR construct were stained with (1) the mAbs C40-PE (Fig. 2B, left panels); (2) the ME20.4 mAb followed by an anti-mouse-PE (Fig. 2B, middle panels); (3) the ME20.4 mAb-MicroBead complex followed by an anti-MicroBead-PE reagent (Labeling Check Reagent, Miltenyi; Fig. 2B, right panels). The results clearly showed that NWL-expressing CAR T cells were recognized by all the combinations tested (Fig. 2B, upper panels). Concerning the NWN2 construct (lower panels), the ME20.4 mAb was able to bind the transduced cells and can be in turn recognized by an anti-mouse mAb (lower middle panel), thus justifying the successful selection obtained with the two-step procedure. On the contrary, when directly coupled to the MicroBeads, the ME20.4 mAb is no more able to bind the NWN2 CAR (right lower panel), thus suggesting the presence of a steric hindrance affecting the access to the epitope when the antibody is coupled too close to the beads. Of note, these results demonstrate the applicability of a clinically validated selection process<sup>11,12</sup> (ClinicalTrials.gov, NCT00423124) to the manufacturing of CAR T cells endowed with an NWN2 spacer.

To characterize the T cell memory differentiation of lymphocytes transduced with the original NWL and NMS variants<sup>10</sup> and with the new NWN4, NWN3, and NWN2 chimeras, purified CAR T cells were analyzed by FACS for the expression of the CD45RA and CD62L markers (Supplementary Fig. S2). CD44v6-NWN3 and CD44v6-NWN4 CAR T cells showed a differentiation profile similar to the CD44v6-NWL.CAR T cells ( $T_{SCM}$ -like cells 39%, 34%, and 41%, respectively), whereas CD44v6-NWN2.CAR T cells had a less differentiated phenotype, with a percentage of  $T_{SCM}$ -like cells similar to CD44v6-NMS.CAR T cells (54%, 59%, respectively). These results suggest that modification of the spacer region in the CD44v6.CAR molecule may impact on the differentiation of memory T cells.

Memory phenotype dictates the self-maintenance capacity of tumor-specific T cells<sup>4,27</sup> impacting on clinical outcome. Therefore, the CD44v6-NWN2.CAR construct was in the first instance selected for further functional *in vitro* and *in vivo* studies. CAR T cells manufactured from several donors ( $n=8$ ) were characterized for CAR expression and memory phenotypes (Fig. 3). In agreement with the reported results,<sup>10</sup> we observed a difference in the expression level of the various CARs (NWL>NWN2>NMS; Fig. 3A). The analysis of T cell differentiation (Fig. 3B), performed in multiple experiments, confirmed the results previously observed with CD44v6-NWN2.CAR T cells (Supplementary Fig. S2A), showing an earlier differentiation profile compared with CD44v6-NWL.CAR T cells, which paralleled the lower expression trend of the exhaustion markers PD1, LAG3, and TIM3 (Supplementary Fig. S2B).

It has been reported that, depending on the CAR construct, variable extents of tonic signaling may occur in CAR T cells,<sup>28,29</sup> which can induce T cell differentiation.<sup>30</sup> To investigate the possible factors underlying the observed differences in CAR expression and memory phenotype, we performed biochemical analysis of the cell surface-expressed CAR molecules, and of their activation in basal conditions. Cell surface proteins from CD44v6.CAR T cells at the end of the manufacturing process (*i.e.*, day 10) were purified and analyzed. As reported in Fig. 4A and B, the expression level of the different CD44v6.CARs on the cell surface (pull-down fraction) showed the same pattern (NWL>NWN2>NMS) observed by cytofluorimetric analysis with the anti-LNGFR mAb. Interestingly, the CD44v6-NMS.CAR was expressed at high levels in the cells (total lysate), but remained in the unbound fraction that is representative of the intracellular compartment. A possible explanation of this behavior comes from the SDS-PAGE analysis performed in nonreducing conditions, showing that the CD44v6-NMS.CAR is prevalently present in the cells as a homodimer with covalent bonds (Fig. 4E), a conformation that is probably retained in the cells. Actually, the analysis of all the CD44v6.CARs indicated that the progressive shortening of the spacer correlated with an increase in the formation of covalently bound homodimer (Fig. 4E).

Next, we evaluated the phosphorylation level of the different CD44v6.CARs present on the cell surface. The relative quantity of the phosphorylated CARs present in the pull-down fraction (Fig. 4C, D) paralleled the relative quantity of the corresponding total CARs present on the cell membrane (Fig. 4B). Indeed, the ratios between the densitometric value of phosphorylated and total form for each CAR were identical. These results indicate that the NWL, NWN2, and NMS CARs have the same level of phosphorylation. CD44v6-NWL.CAR T cells, showing a higher expression of CARs on the cell surface, were therefore characterized by an enhanced tonic signaling, which could be responsible for their more differentiated phenotype.

The intrinsic phosphorylation observed for the CD44v6.CARs could be due, at least partially, to the recognition of the target antigen expressed on activated T lymphocytes. However, murine T lymphocytes expressing the human CAR showed CAR phosphorylation despite the fact that the CD44v6 scFv does not recognize the murine CD44v6 antigen (Fig. 4F), thus suggesting that the antigen-dependent mechanisms could have only a minimal, if any, impact on the basal level of CAR phosphorylation observed.

Altogether, these results support the hypothesis that the effects of the LNGFR spacer length on CAR T cell differentiation are at least partly mediated by modulation of the amount of CAR molecules reaching the cell membrane.

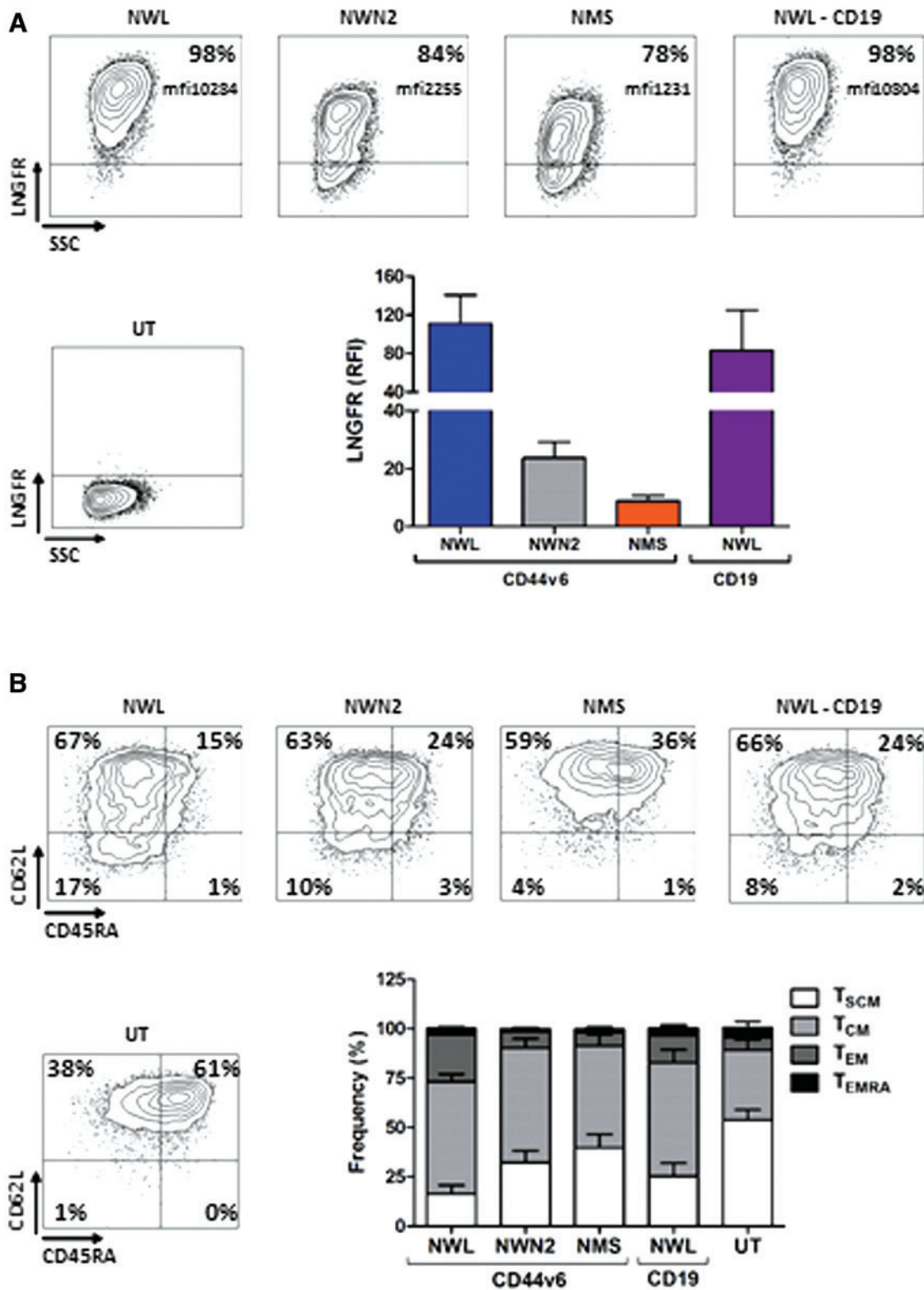


**Figure 3.** Characterization of CD44v6.CAR T cells used for functional analysis. **(A)** CAR expression in transduced T lymphocytes detected with the anti-LNGFR mAb C40-1457. Plots of a representative experiment are shown on the left. On the right, means with SDs of the results obtained with eight independent donors are shown. Paired *t*-test on LNGFR expression was statistically significant for CD44v6-NWN2 ( $p \leq 0.05$ ) and CD44v6-NMS ( $p \leq 0.05$ ) compared with CD44v6-NWL cells. **(B)** T cell memory phenotype was defined based on CD45RA and CD62L expression at day 10 after transduction. Plots of a representative donor are shown on the left. On the right, means with SDs of the results obtained with eight independent donors are shown. Paired *t*-test on  $T_{SCM}$  was statistically significant for untransduced (UT;  $p \leq 0.0001$ ), CD44v6-NWN2 ( $p \leq 0.001$ ), CD44v6-NMS ( $p \leq 0.001$ ), and CD19-NWL ( $p \leq 0.01$ ) cells, compared with CD44v6-NWL cells.  $T_{SCM}$  (CD45RA<sup>+</sup>/CD62L<sup>+</sup> memory stem T cells),  $T_{CM}$  (CD45RA<sup>-</sup>/CD62L<sup>+</sup> central memory T cells),  $T_{EM}$  (CD45RA<sup>-</sup>/CD62L<sup>-</sup> effector memory T cells),  $T_{EMRA}$  (CD45<sup>+</sup>/CD62L<sup>-</sup> effector memory RA T cells). Color images are available online.



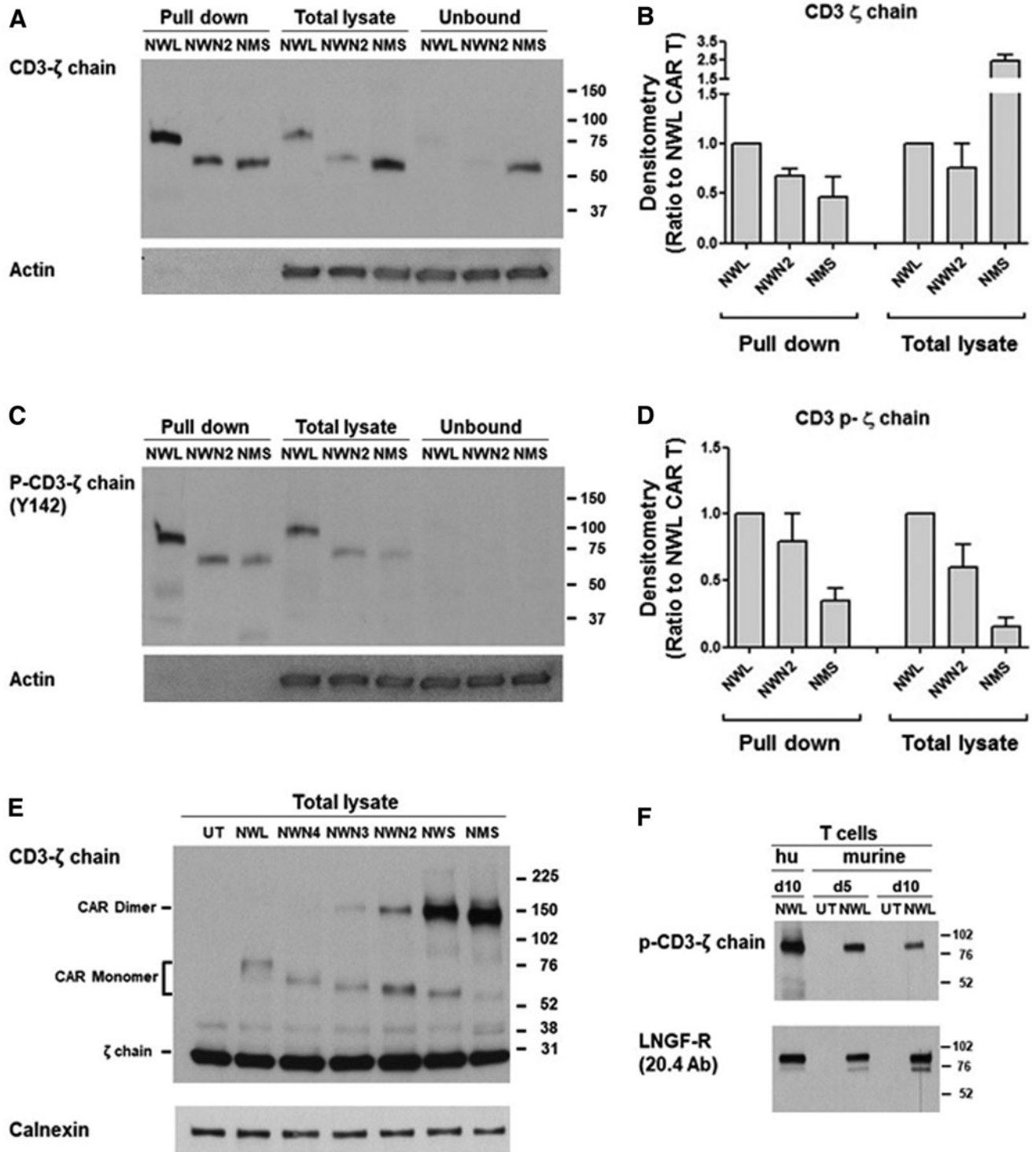


**Figure 4.** Biochemical analysis of the CD44v6.CAR expression and phosphorylation. **(A)** Samples of cell surface protein (pull-down), total lysates, or unbound fractions, from the different CD44v6.CAR T, were immunoblotted with the CD3- $\zeta$  chain Ab, or actin as loading control. A representative experiment out of two is shown. **(B)** Densitometric analysis of the bands shown in **A** from two experiments performed with different donors was performed and results were expressed as ratio to the CD44v6-NWL.CAR T (mean  $\pm$  SE). **(C)** Samples of cell surface protein (pull-down), total lysates, or unbound fractions, from the different CD44v6.CAR T, were immunoblotted with the anti-phospho-CD3- $\zeta$  chain (Tyr142) Ab, or actin as loading control. A representative experiment out of three is shown. **(D)** Densitometric analysis of the bands shown in **C** from two experiments performed with different donors was performed and results were expressed as ratio to the CD44v6-NWL.CAR T (mean  $\pm$  SE). **(E)** Total lysates from CD44v6.CAR T cells were analyzed by immunoblotting with the anti CD3- $\zeta$  chain Ab in nonreducing conditions, and normalization was performed on the same filter by calnexin blot. A representative experiment out of three is shown. **(F)** Total lysates from murine (at day 10 or 15 of culture) or human (hu; day 10) CD44v6-NWL.CAR T cells were analyzed by immunoblotting with the anti-phospho-CD3- $\zeta$  chain (Tyr142) Ab. Normalization was obtained by LNGFR immunoblotting. A representative experiment out of two is shown.

### Functionality of CD44v6 CAR T cells *in vitro*

The functionality of CD44v6.CAR T cells endowed with the different CAR constructs was investigated testing their activation and cytotoxic activity against tumor cell lines expressing different levels of CD44v6: MR232 (RFI=13.0), MM.1S (RFI=5.6), and IGROV-1 (RFI=2.8). As negative control, CD44v6-negative cell lines were used (MOLT-4 with RFI=1.0).

All three CD44v6.CAR T cells (NWL, NWN2, and NMS) were specifically activated by the CD44v6-positive cell lines tested. Cytokine production (*i.e.*, intracellular TNF- $\alpha$  and IFN- $\gamma$ ), and degranulation, evaluated as CD107a cell surface expression, markedly increased upon incubation with MR232 and IGROV-1 tumor cells (Fig. 5A, B, left panels). The percentage of IFN- $\gamma$ -positive cells was lower but still detectable, probably due to the short time point chosen for the analysis (Supplementary Fig. S3B). The CD44v6-NWN2.CAR T cells showed an activity higher than CD44v6-NMS.CAR T cells and more similar to that of CD44v6-NWL.CAR T cells (Fig. 5A, B, right panels). No activation of CD44v6.CAR T cells was detected in the presence of CD44v6-negative cell lines (data not shown), whereas they showed similar, CAR-independent, functional activity when stimulated by PMA/IONO (Fig. 5A, B, right panels).

To evaluate if the observed CAR T cell activation paralleled the cytotoxic activity, the different CD44v6.CAR T cells were challenged against CD44v6-positive and CD44v6-negative targets (Fig. 5C). As expected, all CD44v6.CAR T cells tested were specifically cytotoxic against CD44v6-positive tumor cell lines (*i.e.*, MR232, MM.1S, and IGROV-1). Interestingly, even if not statistically significant, the CD44v6-NWN2.CAR T cells showed a cytotoxicity higher than CD44v6-NMS.CAR T cells and very close to the CD44v6-NWL.CAR T cells. The cytotoxicity was antigen specific, without off-target activity, as demonstrated by the absence of killing against the CD44v6-negative cell line (MOLT-4), as well as by the lack of cytotoxicity of the CD19-NWL.CAR T cells against the cell lines tested (Fig. 5C), which are CD19 negative.

Altogether, these results indicate that the relative level of activation and cytotoxic activity of the three CD44v6.CAR T cells tested (NWL $\geq$ NWN2>NMS) partially correlates with the level of CAR expression (NWL>NWN2>NMS), as well as with their memory differentiation status (NWL>NWN2 $\geq$ NMS).

Effector T cells are endowed with a more rapid and efficient killing ability compared with naive and memory T cells.<sup>31</sup> To investigate the potential impact of the differentiation status on the cytotoxic activity of CD44v6.CAR T cells, we enriched the effector component of all the CAR T populations under investigation, to obtain similar and therefore comparable phenotypic profiles. At the end of the manufacturing process, CAR T cells were further stimu-

lated by OKT-3 and IL2 for 10 days. After a variable extent of proliferation (Supplementary Fig. S4A), they expressed lower levels of CAR, while maintaining the same relative difference (NWL>NWN2>NMS; Supplementary Fig. S4B), and showed similar CD4 and CD8 cell ratio (Supplementary Fig. S4C) and effector memory profiles (Supplementary Fig. S4D).

In particular, at the end of the manufacturing process (day 10), a portion of CAR T cells from donor HD#87 were maintained in culture and differentiated by stimulation with IL2 and OKT-3 for an additional 10 days. The two samples were then analyzed for memory differentiation (Fig. 6A, C) and tested for their lytic activity against MR232, MM.1S, and IGROV-1 cells at different effector/target ratios (Fig. 6B, D). In these conditions, we observed that the cytotoxic activity of the shorter CAR variants (NWN2 and NMS) was similar to that of CD44v6-NWL.CAR T cells. These results suggest that at the end of the manufacturing process, the *in vitro* killing property of the CAR T cells is related to the amount of effector memory T cells in the product.

### CD44v6.CAR T cell interaction with epitopes proximal or distal to the cell surface

Spacer domains can actively influence CAR T cell functionality both *in vitro* and *in vivo*.<sup>32</sup> Moreover, CARs with long or short spacers better recognize antigens that are proximal or distal to the cell membrane, respectively.<sup>8</sup> The target antigen CD44v6 is expressed on the tumor cell surface as a mixture of CD44v6 molecules of different length, due to its large number of variable exons.<sup>18</sup>

To investigate the behavior of the different CD44v6.CAR T cells when challenged with distal or proximal epitopes, MOLT-4 cells were engineered to express two CD44v6 isoforms cloned from different cell lines (Fig. 7A) and containing variable exon v6 associated with a different number of variable exons. As shown in Fig. 7B, the short CD44v6(v6) isoform expressed by activated T lymphocytes contains only the variable exon v6, which is therefore proximal to the cell membrane. In the long CD44v6(v6-v10) isoform, cloned from the THP-1 cell line, the variable exon v6 is distal to the cell membrane, due to the presence of variable exons v7 to v10. The CD44v6(v6-v10) isoform is mainly expressed by tumor cells<sup>18</sup> and we confirmed that along with other isoforms, it was also expressed by the MR232, MM.1S, and IGROV-1 tumor cell lines used in this study (data not shown).

Retroviral vectors, expressing the two isoforms, were used to transduce the CD44v6-negative MOLT-4 cell line. After selection, the two cell lines showed about 90% of CD44v6 positivity with the same levels of antigen expression (RFI 3.2). These cell lines were used as target cells to investigate the cytolytic activity of the different CAR T cells (Fig. 7C). To avoid misleading results due to the different composition in memory subsets, CAR T cells

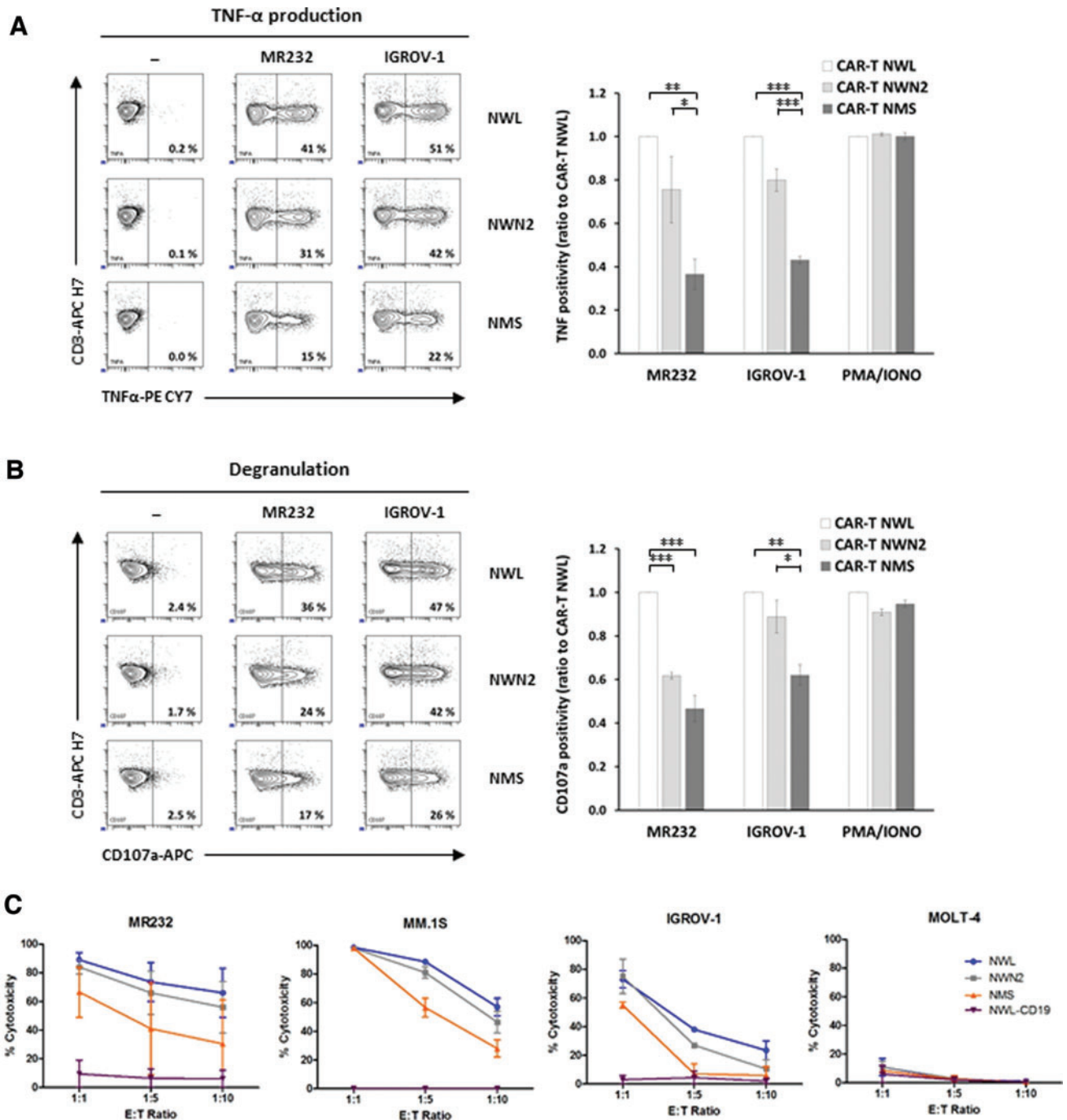


**Figure 5.** Functional analysis of CD44v6 CAR T cells *in vitro*. **(A, B)** Activation of the three CD44v6.CAR T cells (NWL, NWN2, and NMS) was analyzed by coculture with MR232, IGROV-1 (E:T ratio 1:1), or after PMA/ionomycin stimulation (5 h of incubation). Percentage of TNF- $\alpha$ -positive **(A)** or CD107a-positive **(B)** CAR T cells was analyzed by FACS analysis (representative plots on the *left*). The results obtained from three independent donors are shown (mean  $\pm$  SEM) in the graphs, expressed as relative ratio to CD44v6-NWL.CAR T positivity. \* $p < 0.05$ , \*\* $p < 0.01$ , \*\*\* $p < 0.001$  (Bonferroni's multiple comparison test). **(C)** Cytotoxic activity of the three CD44v6.CAR T cells (NWL, NWN2, and NMS) and the CD19-NWL.CAR T cells was analyzed by coculture with the indicated target cells, expressing luciferase, at different ratios. After 24 h, the bioluminescence emitted by the live target cells was detected. The results obtained from two independent donors are shown (mean  $\pm$  SEM). PMA, phorbol myristate acetate. Color images are available online.

were stimulated with OKT-3 and IL2 to obtain comparable populations of effector cells, as previously described. The CD44v6(v6) isoform was recognized by all the CD44v6.CAR T cells tested (Fig. 7C, left panel). In particular, CAR T cells with the shorter spacers (NWN2 and

NMS) showed a higher killing capacity compared with the CD44v6-NWL.CAR T cells.

Interestingly, the CD44v6-NWN2 and CD44v6-NMS.CAR T cells when challenged with MOLT-CD44v6(v6-v10) cells, which have a distal epitope

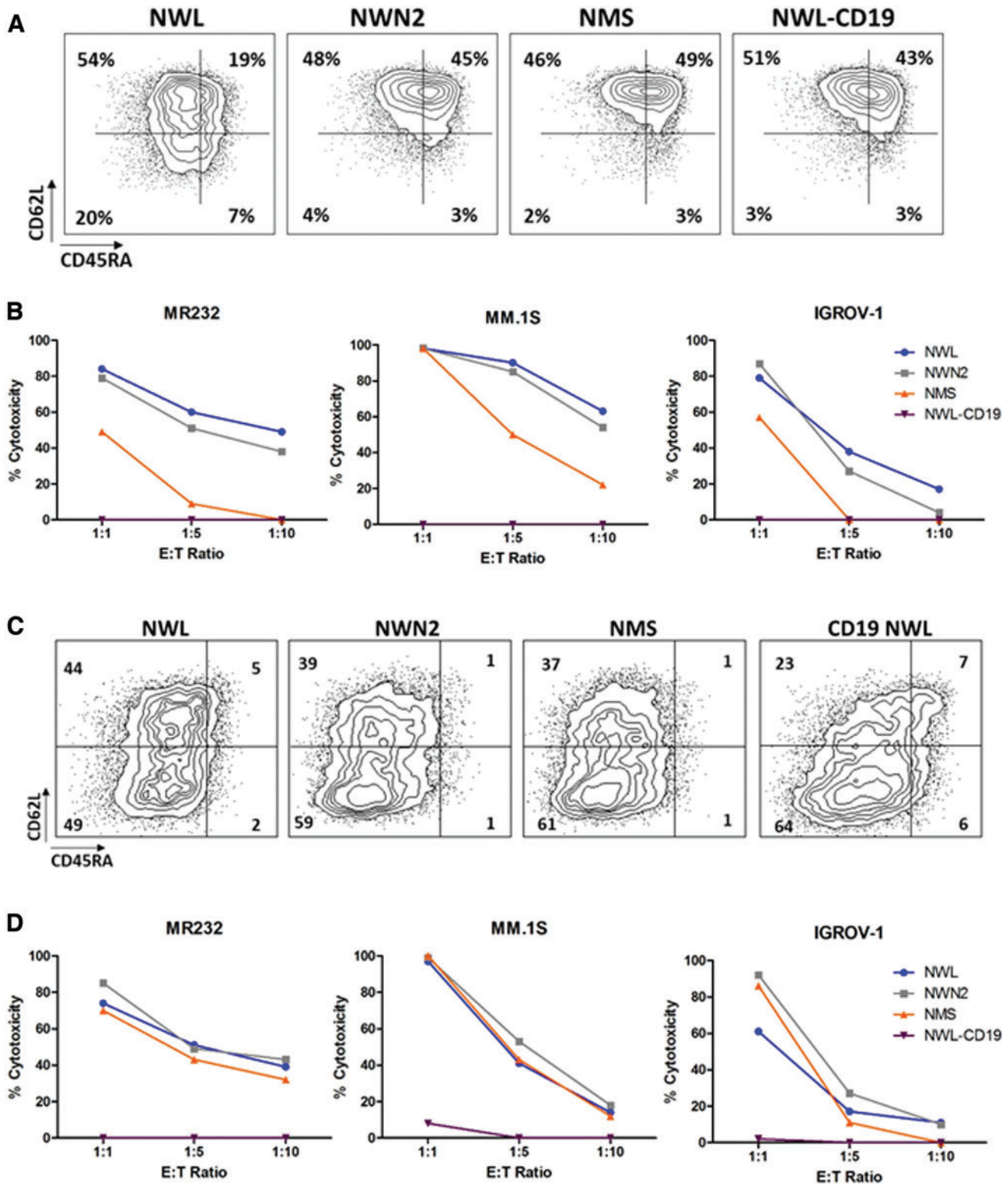


**Figure 6.** Differentiation status influences the cytotoxic activity of CD44v6.CAR T cells. CD44v6.CAR T cells (NWL, NWN2, and NMS) and CD19-NWL.CAR T cells were kept early differentiated (**A**) or *in vitro* differentiated (**C**) with IL2 (100 U/mL) and OMT-3 (30 ng/mL), and their memory phenotype was defined by CD45RA and CD62L expression. T<sub>SCM</sub> (CD45RA<sup>+</sup>/CD62L<sup>+</sup> memory stem T cells), T<sub>CM</sub> (CD45RA<sup>-</sup>/CD62L<sup>+</sup> central memory T cells), T<sub>EM</sub> (CD45RA<sup>-</sup>/CD62L<sup>-</sup> effector memory T cells), T<sub>EMRA</sub> (CD45<sup>+</sup>/CD62L<sup>-</sup> terminally differentiated T cells). Results obtained from a representative donor are shown. Cytotoxic activity of the early differentiated (**B**) or differentiated (**D**) CAR T cells was analyzed after 24 h of coculture with the MR232, MM.1S, and IGROV-1 target cells at the indicated E:T ratio. Results obtained from a representative experiment out of two from independent donors are shown. Color images are available online.

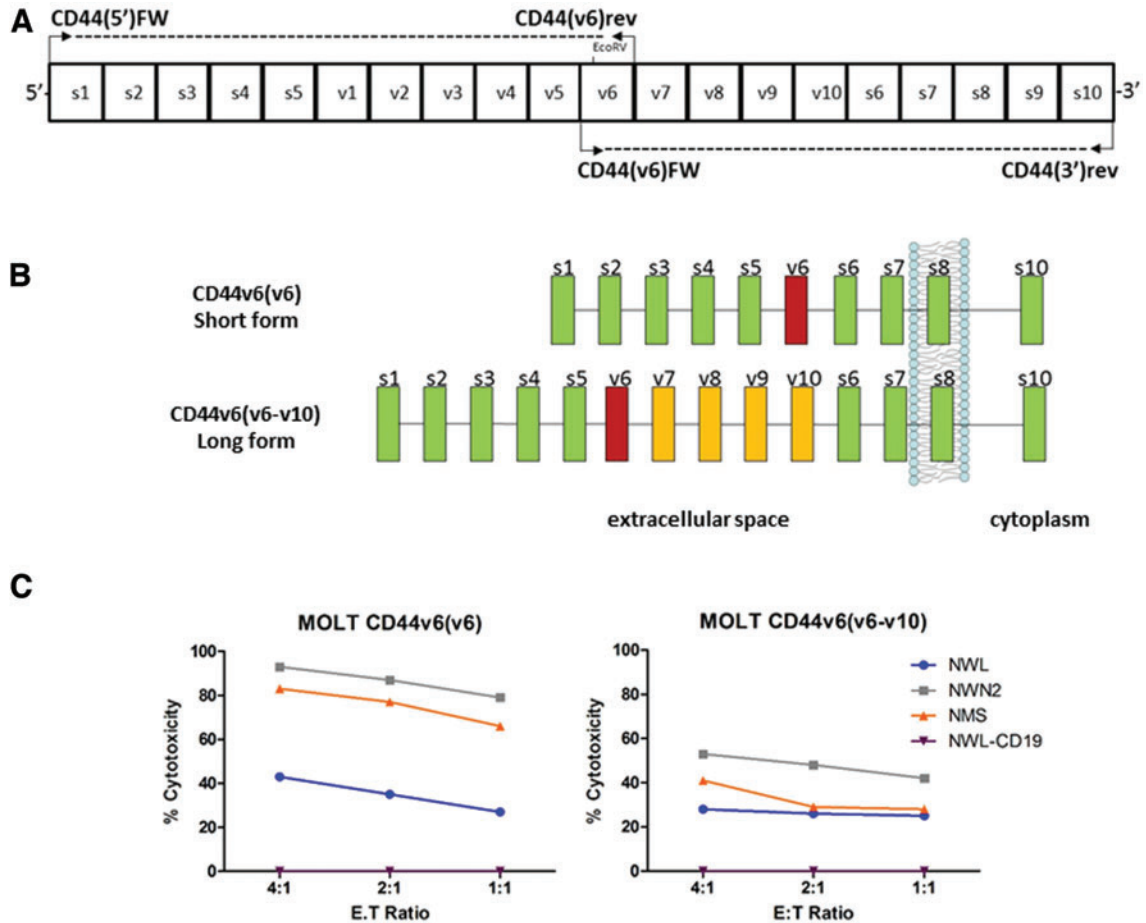


**Figure 7.** Cloning of two CD44v6 isoforms. **(A)** Schematic representation of the coding region of human *CD44* gene (s1-s10: standard exon; v1-v10: variant exon) and localization of the primers used to amplify the CD44 transcripts. **(B)** Schematic representation of CD44 and CD44v6 cloned isoforms: CD44v6(v6) from activated T lymphocytes, CD44v6(v6-v10) from THP-1. Box color code: *green* indicates standard exons; *yellow* indicates variable exons; *magenta* indicates variable exon 6. **(C)** Cytotoxic activity of the differentiated CAR T cells was assessed by coculture with MOLT-CD44v6(v6) or MOLT-CD44v6(v6-v10), at the indicated E:T ratio. Results obtained from a representative experiment out of two from independent donors are shown (mean  $\pm$  SEM). Color images are available online.

showed a decreased activity, reaching killing levels close to those of the CD44v6-NWL.CAR T cells (Fig. 7C, right panel). These results suggest that the LNGFR spacer can be tailored to proximal and distal epitopes. In particular, we observed an improved interaction with antigen proximal to the plasma membrane with the CD44v6-NWN2 chimera.

#### CD44v6-NWN2.CAR T cells mediate *in vivo* antitumor activity in xenogenic models of hematological and solid tumors

In preclinical studies, the infusion of early differentiated T cells results in greater cell expansion, persistence, and tumor destruction.<sup>4,27</sup> Moreover, in clinical trials, CAR T persistence has been associated with a positive clinical outcome. On this ground, the antitumor activity of CD44v6.CAR T cells bearing different spacers was tested *in vivo* in xenogeneic models of AML and ovary carcinoma. NOD/SCID/IL2Rnull (NSG) mice were infused intravenously (iv) with CD44v6-positive THP-1 leukemia

cells and, after 14 days when high leukemia burden developed, were treated with CD44v6.CAR T cells (NWL, NWN2) or the CD19-NWL.CAR T cells as control. Liver weights, as a measure of tumor burden, were evaluated at sacrifice (6 weeks). As expected, mice treated with both CD44v6.CAR T cells showed a better antitumor response compared with mice treated with CD19-NWL.CAR T cells, as indicated by the lower liver weight at sacrifice (Fig. 8A). Moreover, CD44v6-NWN2.CAR T cells showed a superior ability to control leukemia progression with respect to CD44v6-NWL.CAR T cells.

Recently, we demonstrated that CD44v6.CAR T-based adoptive therapy led to tumor growth control in human ovarian and lung carcinoma models,<sup>15</sup> and therefore, we investigated CD44v6-NWN2.CAR T antitumor activity in the CD44v6-positive IGROV-1 ovarian carcinoma model.

Following our well-established protocol,<sup>15</sup> NSG mice ( $n=5$ /group) were implanted subcutaneously with  $3 \times 10^5$  IGROV-1 cells, 6 days later were infused iv with  $4.5 \times 10^6$  CD44v6-NWN2.CAR T cells and monitored for survival.

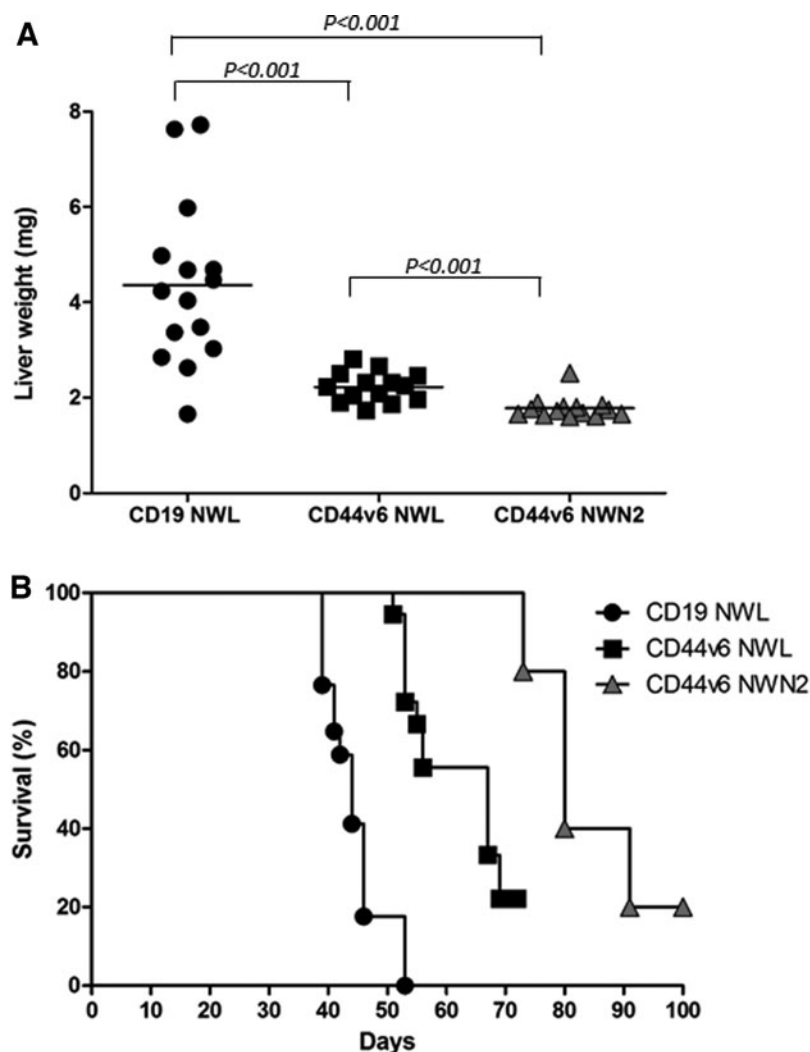


**Figure 8.** *In vivo* antitumor activity. **(A)** CD44v6 CAR T cell-mediated antileukemic effect was evaluated in the well-established THP-1 high-burden disease model. Liver weight (mg) in the different treatment groups at sacrifice (6 weeks) is shown ( $n=3$  independent experiments with different T cell donors). Results from paired *T* test are shown. **(B)** NSG mice were subcutaneously injected with  $3 \times 10^5$  CD44v6<sup>+</sup> IGROV-1 tumor cells. Seven days later, mice were infused via tail vein injection with  $4.5 \times 10^6$  CD19 or CD44v6.CAR T cells and tumor growth quantified by measuring tumor size. Mice treated with CD44v6-NWN2.CAR T cells showed an enhancement of survival several weeks after treatment compared with CD19-NWL.CAR T mice ( $n=17$ ;  $p \leq 0.0002$ ), as well as with CD44v6-NWL.CAR T ( $n=18$ ;  $p \leq 0.0075$ ). Results from log-rank test are reported.

The results were compared with the historical data reported in Porcellini *et al.*<sup>15</sup> As shown in Fig. 8B, CD44v6-NWN2.CAR T cells were able to extend overall survival, more efficiently than CD44v6-NWL.CAR T cells ( $p \leq 0.0075$ ).

Altogether, the data obtained in the two tumor models suggest that the changes introduced in the spacer region of the CD44v6-NWN2 CAR improve CAR T antitumor efficacy.

## DISCUSSION

Optimization of CAR design and choice of appropriate target antigens are mandatory for a successful CAR-mediated therapy. Research studies in CAR design mainly

focused on identifying scFvs that confer recognition of malignant cells without serious toxicity on normal tissues, as well as on defining optimal intracellular signaling modules to activate T cell effector functions. In addition, target recognition by CAR T cells is strongly affected by the length and composition of the spacer sequences between the scFv and the T cell membrane. Indeed, differences of spacer length resulted in different antitumor effects,<sup>9,33</sup> and spacers derived from the IgG1 hinge-CH<sub>2</sub>CH<sub>3</sub> caused detrimental effects in a xenograft leukemia model, due to the presence of an Fc- $\gamma$  receptor binding motif.<sup>34</sup> To address this issue, CARs containing different LNGFR-derived spacers were developed.<sup>10</sup> Human T cells expressing the CD44v6-NWL.CAR with the longer LNGFR spacer form were demonstrated to be functional

both *in vitro* and *in vivo*,<sup>10</sup> as well as selectable by well-validated clinical-grade processes,<sup>11–13</sup> based on the use of mAbs that do not impact on the activation status of the CAR T cells.<sup>35</sup>

A second CD44v6.CAR endowed with a short and mutated LNGFR spacer, (*i.e.*, LNGFR mutated short, NMS),<sup>10</sup> while being functional, was not immunoselectable with the available technology,<sup>11–13</sup> and therefore, its clinical translation was not further pursued.

These data suggested that the molecular structure of the LNGFR used as spacer is suitable for modifications to modulate the interaction of CAR T cells with the target antigen, to enhance their activity and improve their manufacturing process. In this study, we developed three CD44v6.CARs endowed with new LNGFR spacers of different lengths: NWN4 (200 aa), NWN3 (187 aa), and NWN2 (173aa).

To predict the effectiveness of the various CARs, we evaluated several functional parameters of the purified CAR T cells at the end of the 10-day manufacturing process. In particular, we monitored the level of CAR expression, CAR T cell differentiation with the CD45RA and CD62L markers of memory cells, *in vitro* and *in vivo* antitumor activity, and ability to recognize distal and proximal epitope.

Human T lymphocytes, transduced with the shorter variant (*i.e.*, CD44v6-NWN2.CAR), can be selected with purity  $\geq 90\%$ , by a two-step clinically validated manufacturing process.<sup>11</sup> Interestingly, we demonstrated by biochemical analysis that modifications of the LNGFR spacer length bring differences in the cell surface expression level of CARs, due to intracellular retention of the shorter variants. Shortening the serine/threonine-rich stalk of the LNGFR spacer, which is the site of multiple glycosylations, may have induced changes in the glycosylation pattern possibly reflecting on the conformation and leading to CAR retention in the intracellular compartment, as found for other membrane proteins.<sup>36</sup> This hypothesis is supported by the finding that modifications of the O-linked glycans, present in the stalk of the original LNGFR, produce effects on the LNGFR structure.<sup>37</sup> Moreover, we observed an increased formation of covalently bound homodimers that parallel the progressive shortening of the spacer, and correlate with the intracellular accumulation of the shorter CAR variants. CAR homodimerization caused by structure modifications has already been reported and was correlated with improved T cell activation.<sup>38</sup> CAR clustering is also generally associated with CAR activation.<sup>39</sup> However, the CD44v6-NWL.CAR, which is exclusively composed by the monomeric form when analyzed by SDS-PAGE in nonreducing conditions, is fully functional, in agreement with recent results showing that monomeric CARs remain capable of ligand-mediated CAR cluster formation and signaling.<sup>40</sup>

To *in vitro* characterize the functional activity of the different CD44v6.CAR T cells, we carried out activation and cytotoxic assays using target cell lines from hematological or solid tumors, naturally expressing different levels of the CD44v6 antigen. The CD44v6-NWN2.CAR T cells showed antigen-specific activation and cytotoxic activity comparable with that of CD44v6-NWL.CAR T cells, and higher than that of CD44v6-NMS.CAR T cells. The observed difference seems to be related to the differentiation status of the CAR T cells. Indeed, CAR T cell populations consisting of comparable amounts of effector memory cells showed similar cytotoxic activity against CD44v6-positive target cells.

Efficiency of CAR T cells is also dependent on features of the target cells, including antigen density and the presence of distal or proximal epitope that may influence the efficacy of the CAR T-tumor cell interaction. The impact of spacers of different lengths on recognition of the CD44v6 epitope cannot be evaluated on tumor cells, because these cells express a mixture of CD44v6 proximal and distal epitopes,<sup>18</sup> as the v6 exon can be expressed in association with different patterns of variable exons.

To investigate if the three LNGFR-spacers studied (NWL, NWN2, and NMS), which lengths are different enough to support a distinct interaction with epitopes that are proximal or distal to the cell membrane, confer to the CD44v6.CAR T this capability, we used, as targets, cells expressing one single CD44v6 isoform [*i.e.*, the CD44v6(v6) and CD44v6(v6-v10) isoforms with proximal and distal epitopes, respectively]. Interestingly, we found that CAR T cells with the shorter spacers (NWN2 and NMS) killed more efficiently than the CAR T cells with the longer spacer (NWL) target cells expressing the CD44v6(v6) isoform, whereas the activity was comparable on target cells expressing a more distal epitope [*i.e.*, CD44v6(v6-v10)]. These preliminary results suggest the involvement of stabilization of CAR-mediated immunological synapses in the phenomenon.<sup>41</sup> Indeed, it is known that spacer modification correlates with enhanced cytolytic activity,<sup>42</sup> and that spacer length can be tuned to normalize synapse amplitude,<sup>43</sup> thus regulating phosphatase exclusion and allowing a correct CAR phosphorylation.<sup>44</sup>

One parameter influencing the efficacy of CAR T cell therapy is the cell memory phenotype.<sup>45,46</sup> Early differentiation is associated with durable *in vivo* persistence of CAR T cells, which is essential to control tumor in the long term.<sup>47</sup> In the current study, we demonstrated that CD44v6-NWN2.CAR T cells preserve an early differentiated memory phenotype, compared with CD44v6-NWL.CAR T cells, which is probably related to the CAR spacer modifications.

It is known that B and T lymphocytes can have constitutive tonic signaling in the absence of ligands, which can induce partial differentiation.<sup>48,49</sup> Constitutive

CAR-mediated tonic signaling can be caused by several events, including CAR design and density of CARs on the cell membrane.<sup>28–30</sup> Indeed, our results indicate that CD44v6 antigen expression by activated T lymphocytes<sup>50</sup> has only a marginal, if any, role in CAR phosphorylation, thus supporting the presence of tonic signaling in the CD44v6.CAR T cells, and the hypothesis that the early-differentiated memory phenotype of the CD44v6-NWN2.CAR T cells could be related to the lower level of CAR expression on the cell surface leading to a poor tonic signaling.

Overall, the CD44v6-NWN2.CAR T cells, for the preserved cytotoxic activity of the effector memory cells, and their early memory phenotype have the best features for a superior *in vivo* performance. In agreement, the CD44v6-NWN2.CAR T cells, in both hematological and solid tumor models, showed a better control of tumor growth prolonging overall survival of treated mice.

CD44v6.CAR T cells endowed with an NWN2 spacer possess most features suggestive of a potentially successful clinical translation. Indeed, the transduced cells can be selected with a clinically validated process<sup>11,12</sup> to obtain highly enriched populations of CAR-expressing cells with an early differentiation phenotype and able to exert antitumor activity in both *in vitro* and *in vivo* pre-clinical models.

In conclusion, our data confirm with the modular LNGFR-spacer that an optimal CAR design must consider, besides the scFv affinity and the costimulatory signal, the best spacer length/feature to modulate the performance,

functionality, and persistence of the CAR bearing T cells, within the perspective of its specific application.

## ACKNOWLEDGMENTS

The phase I/IIa clinical trial assessing the safety, feasibility, and efficacy of CD44v6.CAR T cell immunotherapy in patients affected by CD44v6-positive AML and MM (clinical trial.gov NCT04097301) is supported by the European Union's Horizon 2020 research and innovation program under grant agreement 733297.

## AUTHOR DISCLOSURE

C.S., C.A., and S.P. were MolMed employees. A.S., B.V., C.S., D.Z., Y.M.D.L.T., S.C., and C.T. are AGC Biologics SpA (formerly MolMed SpA) employees. AGC Biologics SpA (formerly MolMed SpA) is the applicant of patents on CAR molecules containing LNGFR-derived spacers including the CD44v6-targeted CARs studied in this work.

## FUNDING INFORMATION

No funding was received for this article.

## SUPPLEMENTARY MATERIAL

Supplementary Figure S1  
Supplementary Figure S2  
Supplementary Figure S3  
Supplementary Figure S4

## REFERENCES

- Sadelain M, Riviere I, Brentjens R. Targeting tumours with genetically enhanced T lymphocytes. *Nat Rev Cancer* 2003;3:35–45.
- Ho WY, Blattman JN, Dossett ML, et al. Adoptive immunotherapy: engineering T cell responses as biologic weapons for tumor mass destruction. *Cancer Cell* 2003;3:431–437.
- Jafarzadeh L, Masoumi E, Fallah-Mehrjardi K, et al. Prolonged persistence of chimeric antigen receptor (CAR) T cell in adoptive cancer immunotherapy: challenges and ways forward. *Front Immunol* 2020;11:702.
- Sabatino M, Hu J, Sommariva M, et al. Generation of clinical-grade CD19-specific CAR-modified CD8+ memory stem cells for the treatment of human B-cell malignancies. *Blood* 2016;128:519–528.
- van der Stegen SJ, Hamieh M, Sadelain M. The pharmacology of second-generation chimeric antigen receptors. *Nat Rev Drug Discov* 2015;14:499–509.
- Ghorashian S, Kramer AM, Onuoha S, et al. Enhanced CAR T cell expansion and prolonged persistence in pediatric patients with ALL treated with a low-affinity CD19 CAR. *Nat Med* 2019;25:1408–1414.
- Ramakrishna S, Highfill SL, Walsh Z, et al. Modulation of target antigen density improves CAR T-cell functionality and persistence. *Clin Cancer Res* 2019;25:5329–5341.
- Guest RD, Hawkins RE, Kirillova N, et al. The role of extracellular spacer regions in the optimal design of chimeric immune receptors: evaluation of four different scFvs and antigens. *J Immunother* 2005;28:203–211.
- Hudecek M, Sommermeyer D, Kosasih PL, et al. The non-signaling extracellular spacer domain of chimeric antigen receptors is decisive for *in vivo* antitumor activity. *Cancer Immunol Res* 2015;3:125–135.
- Casucci M, Falcone L, Camisa B, et al. Extracellular NGFR spacers allow efficient tracking and enrichment of fully functional CAR-T cells co-expressing a suicide gene. *Front Immunol* 2018;9:507.
- Ciceri F, Bonini C, Marktel S, et al. Antitumor effects of HSV-TK-engineered donor lymphocytes after allogeneic stem-cell transplantation. *Blood* 2007;109:4698–4707.
- Ciceri F, Bonini C, Stanghellini MT, et al. Infusion of suicide-gene-engineered donor lymphocytes after family haploidentical haemopoietic stem-cell transplantation for leukaemia (the TK007 trial): a non-randomised phase I–II study. *Lancet Oncol* 2009;10:489–500.
- La Seta Catamancio S, Cota M, Arnaudova R, et al. Automated manufacturing process for the production of genetically modified lymphocytes (Abstract 462). *Mol Ther* 2015;23:S183–S184.
- Oliveira G, Ruggiero E, Stanghellini MT, et al. Tracking genetically engineered lymphocytes long-term reveals the dynamics of T cell immunological memory. *Sci Transl Med* 2015;7:317ra198.



15. Porcellini S, Asperti C, Corna S, et al. CAR T Cells Redirected to CD44v6 control tumor growth in lung and ovary adenocarcinoma bearing mice. *Front Immunol* 2020;11:99.
16. Sherman L, Sleeman J, Herrlich P, et al. Hyaluronate receptors: key players in growth, differentiation, migration and tumor progression. *Curr Opin Cell Biol* 1994;6:726–733.
17. Wang Z, Zhao K, Hackert T, et al. CD44/CD44v6 a reliable companion in cancer-initiating cell maintenance and tumor progression. *Front Cell Dev Biol* 2018;6:97.
18. Heider KH, Kuthan H, Stehle G, et al. CD44v6: a target for antibody-based cancer therapy. *Cancer Immunol Immunother* 2004;53:567–579.
19. Casucci M, Nicolis di Robilant B, Falcone L, et al. CD44v6-targeted T cells mediate potent antitumor effects against acute myeloid leukemia and multiple myeloma. *Blood* 2013;122:3461–3472.
20. Verel I, Heider KH, Siegmund M, et al. Tumor targeting properties of monoclonal antibodies with different affinity for target antigen CD44V6 in nude mice bearing head-and-neck cancer xenografts. *Int J Cancer* 2002;99:396–402.
21. Akisik E, Bavbek S, Dalay N. CD44 variant exons in leukemia and lymphoma. *Pathol Oncol Res* 2002;8:36–40.
22. Miller AD, Rosman GJ. Improved retroviral vectors for gene transfer and expression. *Biotechniques* 1989;7:980–982, 984–986, 989–990.
23. Villablanca EJ, Raccosta L, Zhou D, et al. Tumor-mediated liver X receptor- $\alpha$  activation inhibits CC chemokine receptor-7 expression on dendritic cells and dampens antitumor responses. *Nat Med* 2010;16:98–105.
24. Pegoraro L, Matera L, Ritz J, et al. Establishment of a Ph1-positive human cell line (BV173). *J Natl Cancer Inst* 1983;70:447–453.
25. Betts MR, Brenchley JM, Price DA, et al. Sensitive and viable identification of antigen-specific CD8<sup>+</sup> T cells by a flow cytometric assay for degranulation. *J Immunol Methods* 2003;281:65–78.
26. Bonini C, Ferrari G, Verzeletti S, et al. HSV-TK gene transfer into donor lymphocytes for control of allogeneic graft-versus-leukemia. *Science* 1997;276:1719–1724.
27. Gattinoni L, Klebanoff CA, Palmer DC, et al. Acquisition of full effector function in vitro paradoxically impairs the in vivo antitumor efficacy of adoptively transferred CD8<sup>+</sup> T cells. *J Clin Invest* 2005;115:1616–1626.
28. Long AH, Haso WM, Shern JF, et al. 4-1BB costimulation ameliorates T cell exhaustion induced by tonic signaling of chimeric antigen receptors. *Nat Med* 2015;21:581–590.
29. Frigault MJ, Lee J, Basil MC, et al. Identification of chimeric antigen receptors that mediate constitutive or inducible proliferation of T cells. *Cancer Immunol Res* 2015;3:356–367.
30. Ajina A, Maher J. Strategies to address chimeric antigen receptor tonic signaling. *Mol Cancer Ther* 2018;17:1795–1815.
31. Mascher B, Schlenke P, Seyfarth M. Expression and kinetics of cytokines determined by intracellular staining using flow cytometry. *J Immunol Methods* 1999;223:115–121.
32. Johnson JA, Chang CA, Baldwin ML, et al. Chimeric antigen receptor (CAR) targeted epitope determines optimal CAR spacer length for therapy against medulloblastoma [abstract]. *Cancer Immunol Res* 2019;7:A032.
33. Hudecek M, Lupo-Stanghellini MT, Kosasih PL, et al. Receptor affinity and extracellular domain modifications affect tumor recognition by ROR1-specific chimeric antigen receptor T cells. *Clin Cancer Res* 2013;19:3153–3164.
34. Almasbak H, Walseng E, Kristian A, et al. Inclusion of an IgG1-Fc spacer abrogates efficacy of CD19 CAR T cells in a xenograft mouse model. *Gene Ther* 2015;22:391–403.
35. Bondanza A, Casucci M, Bonini C. Chimeric antigen receptors. In: European Patent Office. 2019.
36. Jayaprakash NG, Suroliya A. Role of glycosylation in nucleating protein folding and stability. *Biochem J* 2017;474:2333–2347.
37. Chapman BS, Eckart MR, Kaufman SE, et al. O-linked oligosaccharide on the 75-kDa neurotrophin receptor. *J Neurochem* 1996;66:1707–1716.
38. Bridgeman JS, Hawkins RE, Hombach AA, et al. Building better chimeric antigen receptors for adoptive T cell therapy. *Curr Gene Ther* 2010;10:77–90.
39. Bridgeman JS, Hawkins RE, Bagley S, et al. The optimal antigen response of chimeric antigen receptors harboring the CD3zeta transmembrane domain is dependent upon incorporation of the receptor into the endogenous TCR/CD3 complex. *J Immunol* 2010;184:6938–6949.
40. Chang ZL, Lorenzini MH, Chen X, et al. Rewiring T-cell responses to soluble factors with chimeric antigen receptors. *Nat Chem Biol* 2018;14:317–324.
41. Xiong W, Chen Y, Kang X, et al. Immunological synapse predicts effectiveness of chimeric antigen receptor cells. *Mol Therapy* 2018;26:963–975.
42. Kunkele A, Johnson AJ, Rolczynski LS, et al. Functional tuning of CARs reveals signaling threshold above which CD8<sup>+</sup> CTL antitumor potency is attenuated due to cell Fas-FasL-dependent AICD. *Cancer Immunol Res* 2015;3:368–379.
43. James SE, Greenberg PD, Jensen MC, et al. Antigen sensitivity of CD22-specific chimeric TCR is modulated by target epitope distance from the cell membrane. *J Immunol* 2008;180:7028–7038.
44. Davis SJ, van der Merwe PA. The kinetic-segregation model: TCR triggering and beyond. *Nat Immunol* 2006;7:803–809.
45. Gattinoni L, Klebanoff CA, Restifo NP. Paths to stemness: building the ultimate antitumor T cell. *Nat Rev Cancer* 2012;12:671–684.
46. Gattinoni L, Speiser DE, Lichterfeld M, et al. T memory stem cells in health and disease. *Nat Med* 2017;23:18–27.
47. Grupp SA, Maude SL, Shaw PA, et al. Durable remissions in children with relapsed/refractory ALL treated with T cells engineered with a CD19-targeted chimeric antigen receptor (CTL019). *Blood* 2015;126:681.
48. Monroe JG. Ligand-independent tonic signaling in B-cell receptor function. *Curr Opin Immunol* 2004;16:288–295.
49. Myers DR, Zikherman J, Roose JP. Tonic signals: why do lymphocytes bother? *Trends Immunol* 2017;38:844–857.
50. Griffioen AW, Horst E, Heider KH, et al. Expression of CD44 splice variants during lymphocyte activation and tumor progression. *Cell Adhes Commun* 1994;2:195–200.

Received for publication August 3, 2020;  
accepted after revision January 27, 2021.

Published online: February 5, 2021.